Role of Dislocation Movement in the Electrical Conductance of Nanocontacts

Tadashi Ishida[1], Kuniyuki Kakushima[2], Teruyasu Mizoguchi[1] & Hiroyuki Fujita[1]

[1]Institute of Industrial Science, University of Tokyo, 4-6-1 Komaba, Meguro, Tokyo 153-8505, JAPAN, [2]Tokyo Institute of Technology, 4259, Nagatsuda, Midori, Yokohama, Kanagawa, 226-8502, JAPAN.

Dislocation is a lattice imperfection of crystalline materials. Dislocation movement is induced during plastic deformation and influences the mechanical properties. Although the role of dislocation in mechanical properties has been well understood, the role of dislocation in electrical properties is completely lacking. Only Matthiessen's rule addresses the electrical influence of dislocations at the macroscale. Here, we show that the electrical conductance change due to dislocations and show their movements through *in situ* observation of a gold nanocontact. The density of the dislocations in the gold nanocontact did not affect the electrical conductance. The repeated and discrete dislocation movements resulted in an electrical conductance oscillation. Our results demonstrate how dislocations and their movements affect electric conductance at the nanoscale. This instability issue will cause a big problem for future electric devices such as ultra low power electric devices and nanowire photovoltaic devices.

Dislocations play an essential role in the plastic deformations of crystalline materials. They prevent the synchronized breakage of bonds between atoms in materials and cause gradual deformation by making the one-by-one breakage of single bonds possible. The mechanical aspect of dislocation behavior has been well documented[1,2]. Conversely, the role of dislocations on electrical properties has been explained only by Matthiessen's rule[3] in which electrical conductivity is decreased by the scattering effect, which is driven by the lattice vibration and the existence of impurities and of dislocations in bulk systems[4]. Namely, only macroscopic models have been proposed. At the nanoscale, electrical conductance follows quantum effects and demonstrates unique properties. Ballistic conduction appears when the size is smaller than the mean free path of electrons[5]. The conductance becomes the product of the quantised conductance, G_0 ($=1/12.8$ kΩ), and the number of atoms[6]. These quantum effects are remarkably important in nanoscale electronics because the electrical conductance of nanostructures is extremely sensitive to deformations and the presence of dislocations, even at the atomic scale[7]. In fact, it was proposed that the dislocations are generated inside a gold nanostructure during the deformation process[8]. Thus, a natural question that arises is the following: how do the dislocation and its movements at the atomic scale statically and dynamically affect the electrical conductance of the gold nanostructure? To the best of our knowledge, there is a lack of experimental evidence regarding the influence of dislocations inside a gold nanostructure on the electrical properties primarily because of the difficulty in controlling dislocations inside nanostructures. For this purpose, we applied *in situ* transmission electron microscopy (TEM) in order to visualize the structural changes and deformation driven by the motion of atoms and dislocations under electrical characterization, leading to the elucidation of the mechanisms of nanoscopic phenomena[9–12]. In this work, we formed dislocations inside a gold nanocontact using an original, newly developed micro-electro-mechanical systems (MEMS) in ultra-high vacuum TEM[13] and investigated the influence of the presence and movement of the dislocations on the electrical conductivity at the gold nanocontact (see S1 online). Our findings expose a new aspect in the development of future electric devices, including non-voatile resistive switching memories[14] and atomic switches[15], ultra low power devices with extremely high speed calculation at the same power consumption of conventional ones[16] and atomically small electrical components[17,18] for the detection of ultra small quantity of molecules[19] and future photovoltaic device with high power generation efficiency[20].

Results

Nano scaled low-angle grain boundary. A gold nanocontact was formed between tips by gentle mechanical contact[21] (see Supplementary S2 and Movie 1 online). Figure 1a shows a TEM image of a gold nanocontact taken at 17 min 32 s after the moment of contact between gold tips. According to the lattice fringe analysis, the image was taken from near <110> in zone axis. Dark dots around 1 nm in size were observed to be periodically located
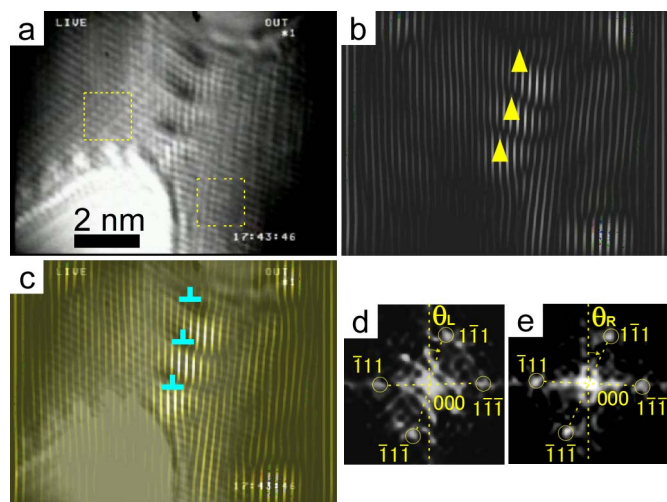
Figure 1 | **Low-angle grain boundary between gold nanograins.** (a) TEM image of the gold nanocontact including dark dots. (b) Fourier-filtered image reconstructed using certain spatial frequencies of the (111) planes. Yellow arrowheads show mismatches of stripes. (c) Overlapped image between a and b. Dark dots correspond to dislocations inside the gold nanocontact, considering the good position agreement between dark dots and mismatch of stripes. (d) FFT image from the left dashed square area in (a). (c) FFT image from the right dashed square area in (a).

at the nanocontact between the gold tips. This dark contrast indicates that strong strains are accumulated around those points. Figure 1b shows the inverted Fourier-filtered (IFF) image reconstructed with selected spatial frequencies of the (111) planes. The yellow arrowheads point to the positions of lattice discontinuities. Figure 1c is an overlaid image of Figures 1a and 1b. From this, we see that the positions of the dark contrasts and the lattice discontinuities are consistent with each other, indicating that dislocations have been formed inside the nanocontact. Moreover, the IFF images of yellow squares in Figure 1a are shown in Figures 1d and 1e. From the IFF images, the tilt angle difference between two grains, θ_L-θ_R, was found to be 8.8 degrees, which is identical to that before the formation of the gold nanocontact in S2. This suggests that the formation of the gold nanocontact did not change the local crystalline orientation. The average distance between neighboring dark dots was found to be approximately 1.5 nm from the TEM image. Assuming that this interface was a low-angle grain boundary with a tilt angle of 8.8 degree, the dislocation distance can be calculated from Frank's equation[22] using the tilt angle and the Burgers vector for gold, 1/2<110> on the (111) plane. The calculated dislocation distance is 1.5 nm. This value is well matched with that in the experimental TEM image. Thus, the dark dots seen inside the gold nanocontact should be considered to be dislocations at the low-angle grain boundary inside the gold nanocontact.

The dislocation density in the gold nanocontact was 2.3×10^{19} m^{-2}, assuming that the gold nanocontact was 6.3 nm in width and 2.1 nm in length. The local dislocation density at the contact area is extremely high, even in comparison to that of strongly deformed bulk materials, $10^{15} \sim 10^{16}$ m^{-2}. Because of this, the effect of dislocations and their movements on the conducatnce of the gold nanocontact should be far more significant in comparison to currently known for the bulk materials.

Conductance oscillation driven by dislocation movements. The movement of dislocations driven by the tensile residual stress inside the nanocontact was traced by TEM observations (Fig. 2, Supplementary Movie 2 online). The loading speed was 0.03 nm/s, and the bias voltage between the tips was 1 mV for the electrical

measurement with suppressing the Joule heating as far as possible. Such an extremely slow loading can be achieved using stable and precise voltage source to control the electrostatic actuator. A micro actuator pulled the nanocontact about 1 nm, and its position was anchored.

The current through the nanocontact was 6.0 μA with 1 mV in bias voltage. The current oscillation started and gradually increased for 0.67 s, even though dislocations remained at their positions (arrowheads a, b in the graph of Fig. 2). The amplitude of current oscillation became saturated to 0.33 μA, and the current ranged from 5.64 to 6.3 μA (arrowhead c in the graph of Fig. 2). At the moment of the maximum amplitude of the current oscillation, 0.67 s from the beginning of the current oscillation, the dislocations suddenly moved and then stopped. The current oscillation continued for 0.7 s after the sudden dislocation movement, and its amplitude decreased during this period (arrowheads d in the graph of Fig. 2). After the current oscillation event, a constant current was measured (arrowheads e in the graph of Fig. 2). Therefore, the data strongly suggest that the current oscillation is correlated with the movement of the dislocations. The conductance change during the current oscillation corresponds to 4 G_0. The number of atoms necessary to induce the current oscillation was assumed to be around 4, considering quantum conductance, which is not far from the observed number of dislocations in the gold nanocontact.

From the *in situ* observation of the nanocontact, the dislocation movement was observed to be synchronous with the current oscillation. The dislocations were initially pinned (Fig. 2a,b). After 0.78 s from the anchorage (Fig. 2c), the dislocations suddenly migrated by 0.23 nm in just 0.07 s, without any pre-event noted from observation. The displacement of the dislocations corresponds to a single lattice plane distance of {111} of gold crystal. After the sudden movements, the dislocations were pinned again to specific locations (Figs. 2d,e). Note that the effect of the electron beam for observation can be taken to be negligible[23–25] (see S3 online).

Electrical conductance independent on number of dislocations. The electrical conductance of the gold nanocontact oscillated whenever dislocations moved inside the gold nanocontact (the timing of the movements was indicated by red arrows in the graph of Fig. 3, Supplementary Movie 3 online). Each cycle of the current oscillation exhibited a similar amplitude and duration at each red arrow at 0.87 s (#1), 2.11 s (#2), 2.57 s (#3), 4.03 s (#4) and 4.56 s (#5). The number of dislocations changed at 2.11 s, indicated by the red arrow #2, due to the dislocation movement from the inside to the outside of the nanocontact, without changing its shape (Figs. 3a–f). Initially, there were 4 dislocations (Figs. 3a,b), which decreased to 3 after 2.11 s (Fig. 3c–f). The dislocation densities of the nanocontact were 3.0×10^{19} m^{-2} with 4 dislocations and 2.3×10^{19} m^{-2} with 3 dislocations. The electrical conductance stayed at 75 G_0, even though the density of dislocations changed. In addition, the amplitude of the current oscillation of the electrical conductance was also independent of the density of dislocations. Interestingly, the amplitude of the current oscillation doubled when the dislocations moved during the second current oscillation at approximately 2.35 s (c in the graph of Fig. 3). The current amplitude doubled due to the overlap between the two oscillations driven by different dislocation movement at 2.11 s, indicated by the red arrow #2, and 2.57 s, indicated by the red arrow #3. During this measurement of the current oscillations, the width of the gold nanocontact and tilt angle between tips remained 4.8 nm and 8.8 degrees, respectively. This result suggests that the density of dislocations inside the gold nanocontact does not affect the electrical conductance; only the dislocation movements affect the electrical conductance.

Discussion

We propose a model to describe the current oscillation due to dislocation movements. According to our observation of the dislocation
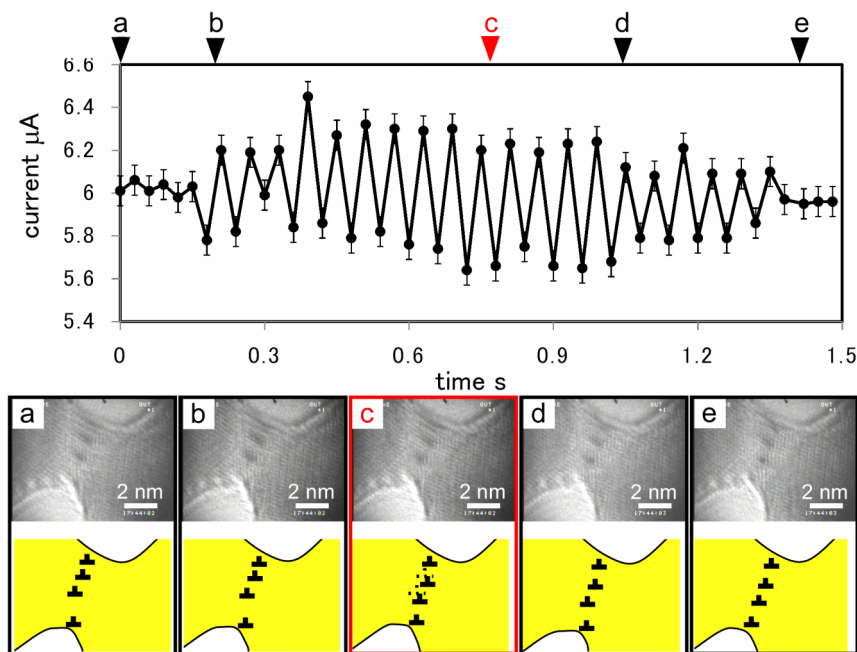
Figure 2 | Electrical current oscillation of the gold nanocontact due to dislocation movement. The current plotted as a function of time shows that the current of the gold nanocontact oscillated for 1.16 s. The error bar is 0.15 µA. Letters in the plot correspond to the images below it. (a–e) TEM images and schematic illustrations of the dislocation movement inside the gold nanocontact. Dislocations are marked with ⊥ in each illustration, and dashed ⊥ marks show the dislocation positions just before the movement. Dislocations remained when the loading of the nanocontact stopped (a). Dislocations did not move when the current through the gold nanocontact started to oscillate 0.21 s after (a) (b). Dislocations moved when the amplitude of the current oscillation was saturated 0.67 s after (b) (c). Dislocations did not move further after the dislocation movement stopped, but the current was observed to continue oscillation for 0.3 s after (c) (d). The current became stable 0.7 s after (c) (e).

movements and the current oscillation, dislocations occurred in the middle of the current oscillations. Some atomic-scale deformations inside the nanocontact should have occurred before and after the dislocation movement because the current oscillation occurred before and after the observed dislocation movements. Gold atoms around dislocations could vibrate to overcome the Peierls energy barrier. Once the path for the dislocation movement was created by these vibrations, the dislocations suddenly moved. After
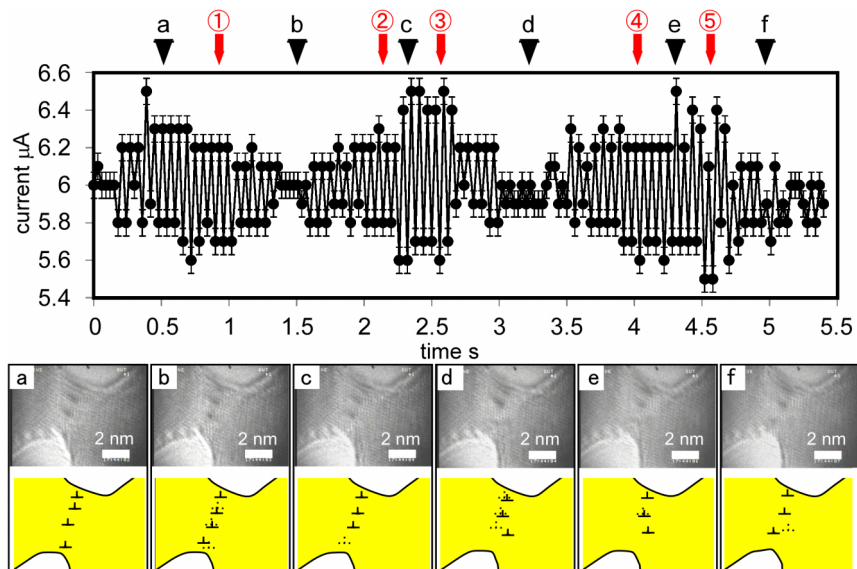

Figure 3 | Relationship between the electrical current and the number of dislocations. The current is plotted as a function of time, and the number of dislocations decreased from 4 to 3 due to the dislocation movements. The current of the gold nanocontact oscillated with each dislocation movement. The error bar is 0.15 µA. Red arrows from 1 to 5 indicate the timing of each dislocation movement. The numbered movements from 1 to 5 occurred at 0.87 s, 2.11 s, 2.57 s, 4.03 s and 4.56 s, respectively. Letters in the plot correspond to TEM images and schematic illustrations. (a–f) Upper images: TEM images of the gold nanocontact including different numbers of dislocations. Lower images: schematic illustrations of the TEM images. Dislocations moved inside the gold nanocontact. The solid dislocation mark indicates the current location of the dislocation. The dashed dislocation mark indicates the previous location of the dislocation before the dislocation movement. (a) 0.51 s, (b) 1.39 s, (c) 2.35 s, (d) 3.23 s, (e) 4.31 s and (f) 4.98 s from the moment when the loading was stopped. The number of dislocations inside the gold nanocontact was 4 (a,b), and the number then decreased to 3 (c–f).

dislocation, gold atoms surrounding the trail of the dislocation movement would have rearranged due to atomic disorder induced by the dislocation movement. Because of these atomic scale fluctuations, the conductance of the gold nanocontact could be modulated, resulting in the observed current oscillation of the conductance of the gold nanocontact.

The dislocation density did not affect the electrical conductance of the gold nanocontact. The conductance of the gold nanocontact with extremely high dislocation density was close in value to that of the gold nanocontact without any dislocations. A few dislocations inside the gold nanocontact consisted of approximately 500 atoms, assuming that the nanocontact was a cylinder packed in a face-centered cubic arrangement[26]. Moreover, the number of free electrons, which are responsible for electrical transport, was 2.3×10^{12} in the nanocontact because the free electron density of gold is 5.9×10^{28} m^{-3} [27]. Thus, the number of dislocations may be considered to be negligibly small in comparison to the number of free electrons in the gold nanocontact.

In summary, we observed the influence of dislocations and their movements on electrical conductivity and found that the density of dislocations in the gold nanocontact did not affect the electrical conductivity but that dislocation movement did. Our findings expose a new aspect in the development of future electric devices.

Methods

Sample preparation and experimental methods. Our experiments were conducted inside an ultra-high vacuum type field emission gun transmission electron microscope (TEM, Hitachi HF2000-UHV) equipped with a specially customised TEM sample holder with 9 electrical feedthroughs for MEMS devices. The TEM was operated at 200 kV, with a lattice resolution around 0.2 nm. The videos showing the low-angle grain boundary of the gold grains at the nano scale were recorded by a high-sensitive Hitachi UTK-2000 television camera at 30 frames per second.

The gold opposing tips with electrostatic actuators were prepared from a silicon-on-insulator (SOI) wafer using bulk-micromachining and focused ion beam (FIB) etching. Aluminum masks for deep reactive ion etching (DRIE) were patterned on both sides of a SOI wafer. DRIE and buffered hydrofluoric acid etching were performed from the backside of the SOI wafer. DRIE was performed from the front side of the SOI wafer. With these fabrication processes, micro electrostatic actuators were obtained. A silicon bridge structure was cut with FIB etching, resulting in silicon opposing tips. Gold was evaporated onto the silicon opposing tips. For details, please refer to the previous publication[13].

Precise and stable control using electrostatic micro actuators. The electrostatic micro actuator integrated in MEMS device was consisted of two parallel electrode plates. The electrostatic force pulls the parallel electrodes and controls the displacement of the electrode when the driving voltage was applied to the electrodes. This electrostatic micro actuator is extremely stable actuation of 0.05 nm in standard deviation in vacuum condition[28]. According to the TEM observation with 0.2 nm in spatial resolution, the displacement can be controlled less than 0.2 nm. The loading speed of the movable tip was controlled by 1 mV step, controlling the driving voltage applied to the electrostatic micro actuators. With this experimental condition, the quite stable and quasi static tensile loading speed of 0.03 nm/s using such stable and accurate actuators achieved.

1. Hirth, J. P. A Brief history of dislocation theory. *Metall. Mater. Trans. A* **16A**, 2085–2090 (1985).
2. Hardwick, D. A. The mechanical properties of thin films: a review. *Thin Solid Films* **154**, 109–124 (1987).
3. Matthiessen, A. On the electric conducting power of the metals. *Philos. Trans. R. Soc. London* **148**, 383–387 (1858).
4. Landauer, R. Spatial variation of current and fields due to localized scatterers in metallic conduction. *IBM J. Res. Dev.* **1**, 223–231 (1957).
5. Wharam, D. A. *et al.* One-dimensional transport and the quantization of the ballistic resistance. *J. Phys. C: Solid State Phys.* **21**, L209–L214 (1988).
6. Landauer, R. Electrical resistance of disordered one-dimensional lattice. *Philos. Mag.* **21**, 863–867 (1970).
7. Ohnishi, H., Kondo, Y. & Takayanagi, K. Quantized conductance through individual rows of suspended gold atoms. *Nature* **395**, 780–783 (1998).
8. Sorensen, M. T., Brandbyge, M. & Jacobsen, K. W. Mechanical deformation of atomic-scale metallic contacts: Structure and mechanics. *Phys. Rev. B* **57**, 3283–3294 (1998).
9. Lagos, M. J. *et al.* Observation of the smallest metal nanotube with a square cross-section. *Nat. Nanotechnol.* **4**, 149–152 (2009).
10. Kiener, D., Hosemann, P., Maloy, S. A. & Minor, A. M. *In situ* nanocompression testing of irradiated copper. *Nat. Mater.* **10**, 608–613 (2011).
11. Ikuhara, Y., Cheng, Y. B., Tatami, J. & Mitomo, M. SIAIONS AND NON-OXIDES, eds.: Kimeya, K., Bing, C. Y. & Tatami, J. **403**, (Trans Tech Publications, Zurich, 2009) p. 43–44.
12. Wen, C.-Y. *et al.* Formation of compositionally abrupt axial heterojunctions in silicon-germanium nanowires. *Science* **326**, 1247–1250 (2009).
13. Ishida, T. *et al.* Design and fabrication of MEMS controlled probes for studying the nano-interface under *in-situ* TEM observation. *J. Micromech. Microeng.* **20**, 075011(8pp) (2010).
14. Sawa, A. Resistive switching in transition metal oxides. *Mater. Today* **11**, 28–36 (2008).
15. Terabe, K., Hasegawa, T., Nakayama, T. & Aono, M. Quantized conductance atomoc switches. *Nature* **433**, 47–50 (2005).
16. Kwok, K. C. & Luong, H. C. Ultra-low-voltage high-performance CMOS VCOs using transformer feedback," *IEEE J. Solid-State Circuits* **40**, 652–660 (2005).
17. Geim, A. K. & Novoselov, K. S. The rise of graphene. *Nat. Mater.* **6**, 183–191 (2007).
18. Yan, H. *et al.* Programmable nanowire circuits for nanoprocessors. *Nature* **470**, 240–244 (2011).
19. Patolsky, F., Zheng, G. & Lieber, C. M. Fabrication of silicon nanowire devices for ultrasensitive, label-free, real-time detection of biological and chemical species. *Nat. Protoc.* **1**, 1711–1724 (2006).
20. Tian, B. *et al.* Coaxial silicon nanowires as solar cells and nanoelectronic power sources. *Nature* **449**, 885–889 (2007).
21. Ishida, T., Kakushima, K. & Fujita, H. Gentle cold welding between gold nano objects driven by electrical field and atomic rearrangement. *J. Appl. Phys.* **110**, 104310 (2011).
22. Frank, F. C. Crystal Dislocations.–Elementary Concept and Definitions. *Philos. Mag.* **42**, 809–819 (1951).
23. Gasga, J. R. & García, R. G. Analysis of the electron-beam radiation damage of TEM samples in the acceleration energy range from 0.1 to 2 MeV using the standard theory for fast electrons. *Radiat. Phys. Chem.* **64**, 359–367 (2002).
24. Iijima, S. *Microclusters*, eds.: Sugano, S., Nishina, Y. & Ohnishi, S. **4** (Springer, Berlin, 1987) pp.186–199.
25. Mikó, Cs. *et al.* Effect of electron irradiation on the electrical properties of fibers of aligned single-walled carbon nanotubes. *Appl. Phys. Lett.* **83**, 4622–4624 (2003).
26. Torquato, S., Truskett, T. M. & Debenedetti, P. G. Is random close packing of spheres well defined? *Phys. Rev. Lett.* **84**, 2064–2067 (2000).
27. Ashcroft, N. W. & Mermin, N. D. *Solid State Physics* (Saunders College Publishing, Orlando, 1976) p.5.
28. Ishida, T., Sato, T., Nabeya, S., Kakushima, K. & Fujita, H. Highly stable spatio-temporal mechanical characterization of nanocontact between sharp tips using electrostatic microactuator inside transmission electron microscope. *Jpn. J. Appl. Phys.* **50**, 077201 (2011).

Author contributions

T.I. carried out TEM experiment and wrote the paper. K.K. contributed to sample preparation and the experiments. T.M. contributed to data analysis, paper writing and revising. H.F. supervised and directed the experiments and the paper writing.

Additional information

Supplementary information accompanies this paper at http://www.nature.com/scientificreports

Competing financial interests: The authors declare no competing financial interests.

How to cite this article: Ishida, T., Kakushima, K., Mizoguchi, T. & Fujita, H. Role of Dislocation Movement in the Electrical Conductance of Nanocontacts. *Sci. Rep.* **2**, 623; DOI:10.1038/srep00623 (2012).